

## Electronic Supporting Information

### **A Dually Responsive Cyanostilbene Derivative for Paper Fluorescence Anti-Counterfeiting and Informational Encryption**

Junxiao Wang<sup>a</sup>, Pengyu Li<sup>a</sup>, Chendong Ji,<sup>a</sup> Junhong Wu<sup>a</sup>, Mingyu Fan<sup>a</sup>, Jun Guan<sup>\*b</sup>, and Meizhen Yin<sup>\*a</sup>

*<sup>a</sup>State Key Laboratory of Chemical Resource Engineering, Beijing Laboratory of Biomedical Materials, Beijing University of Chemical Technology, Beijing 100029 (China)*

*E-mail: yinmz@mail.buct.edu.cn\**

*<sup>b</sup>Key Lab of Organic Optoelectronics & Molecular Engineering, Department of Chemistry, Tsinghua University, Beijing 100084 (China)*

*E-mail: junguan@mail.tsinghua.edu.cn\**

## Materials

All solvents were purchased from commercial suppliers and were directly used as received.

4-Pyridylacetonitrile hydrochloride (98%), 4-Hydroxybenzaldehyde (98%), 4-Methoxyphenylacetonitrile (98%), Benzaldehyde (98%), Benzyl cyanide (98%), all purchased from HEOWNS and used without further purification.

## Characterization

$^1\text{H}$  NMR and  $^{13}\text{C}$  NMR spectra were recorded on a Bruker 400 (400 MHz) spectrometer at room temperature with DMSO- $d_6$  as the solvent and tetramethylsilane (TMS) as the internal standard reference respectively. UV-Vis spectra were obtained on a spectrometer (UV-2600, Shimadzu, Japan). Fluorescence (FL) spectroscopic studies were performed on a fluorescence spectrophotometer (Horiba Jobin Yvon FluoroMax-4 NIR, NJ, USA). ESI-MS were determined by a Waters LCT premier XE spectrometer.

## Test Fluorescence Quantum Yield

The solution of ACN derivatives is obtained upon dissolving the powder in DMSO ( $4 \times 10^{-6}$  M). The powder and test paper is directly placed on the solid sample stand. The absolute quantum yields were measured using integrating sphere on an Edinburgh Instruments FS5 Fluorescence Spectrometer.

## Theoretical calculations

The TD-DFT simulations of the absorbance spectra were carried out with the Gaussian 09 package. The cam-B3LYP functional and the 6-31G\*(d,p) basis set was applied, since it represents a good balance between quality of the results and computational cost.

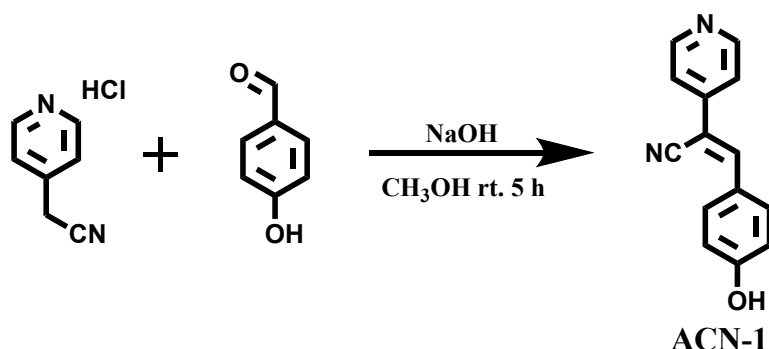
## Preparation of fluorescent paper (FP)

The filter paper is dipping into the THF solution of ACN1 and dries it in the oven forming FP1. The content of ACNs on the filter paper is controlled by modulating the concentration of THF solutions ( $4 \times 10^{-4}$  M and  $2 \times 10^{-3}$  M) forming FP1 and FP1H respectively. The FP2, FP3 and FP4 is obtained by dipping into the ACN2, ACN3 and ACN4 THF solutions with  $2 \times 10^{-3}$  M.

## Preparation of the PBS solution

The solutions of pH 1.0-14.0 are prepared by adding small amounts of hydrochloric acid (0.5 M) or sodium hydroxide (0.5 M) to sodium phosphate buffer solution (0.1 M).

## Synthesis



**Scheme S1.** Structure and synthesis route to ACN1.

**Synthesis of (Z)-3-(4-hydroxyphenyl)-2-(pyridin-4-yl)acrylonitrile (ACN1):** 4-Pyridylacetonitrile hydrochloride (0.3 g, 2 mmol), 4-Hydroxybenzaldehyde (0.29 g, 2 mmol) and NaOH (0.16 g, 4 mmol) were dissolved in 80 ml methanol under stirring at room temperature for 10 hours. Slow neutralization of the mixture with conc. HCl to pH=7 afforded a yellowish precipitate. The mixture is filtrated, washing the filter residue with water 2 times and collect the filter residue. The residue is collected to give ACN1 (0.16 g, 0.2 mmol) yield 30%. <sup>1</sup>H NMR (400 MHz, DMSO-*d*<sub>6</sub>) δ 10.46 (s, 1H), 8.66 (d, J = 6.2 Hz, 2H), 8.20 (s, 1H), 7.94 (d, J = 8.7 Hz, 2H), 7.70 (d, J = 6.2 Hz, 2H), 6.96 (d, J = 8.7 Hz, 2H). <sup>13</sup>C NMR (101 MHz, DMSO) δ 161.21 (s), 150.59 (s), 146.15 (s), 141.95 (s), 132.45 (s), 124.37 (s), 119.66 (s), 117.97 (s), 116.30 (s), 103.33 (s). ESI-MS: Calculated mass: 222.0791; measured: 223.0934.

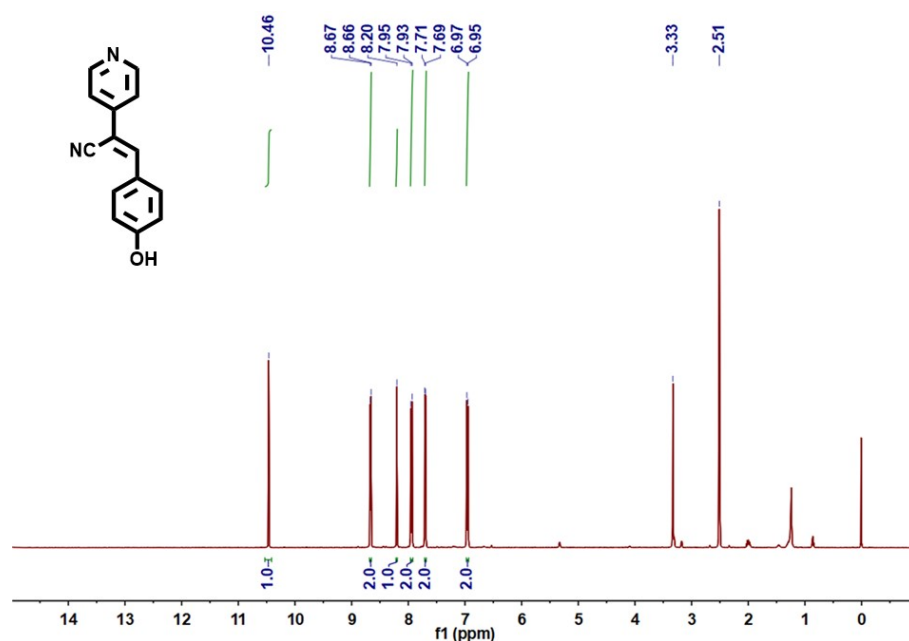


**Figure S1.** <sup>1</sup>H NMR spectrum of ACN1 in DMSO-*d*<sub>6</sub>.

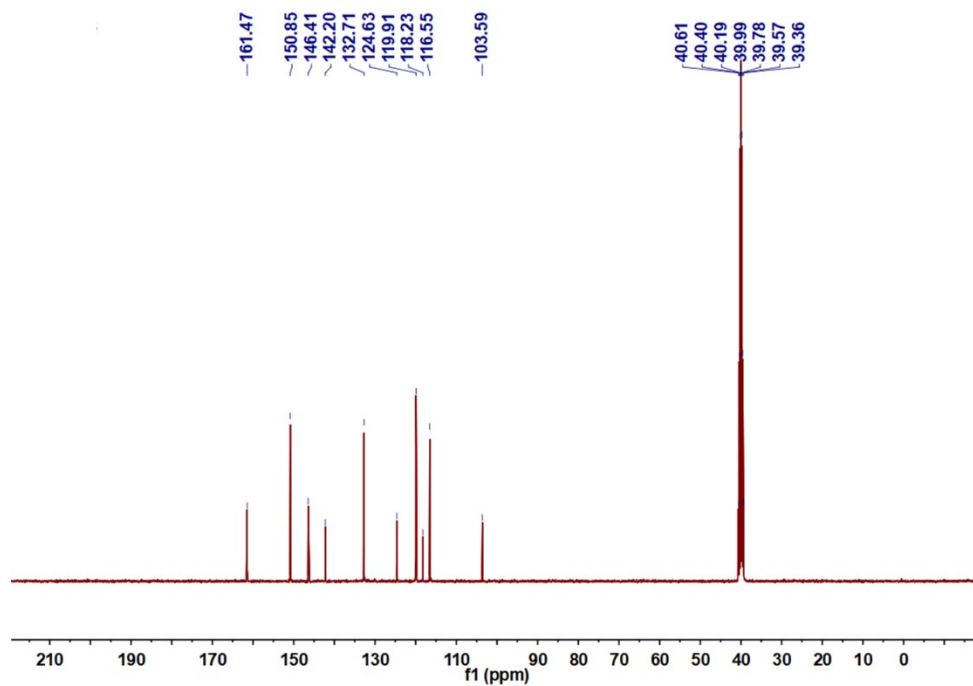


Figure S2.  $^{13}\text{C}$  NMR spectrum of ACN1 in  $\text{DMSO-d}_6$ .

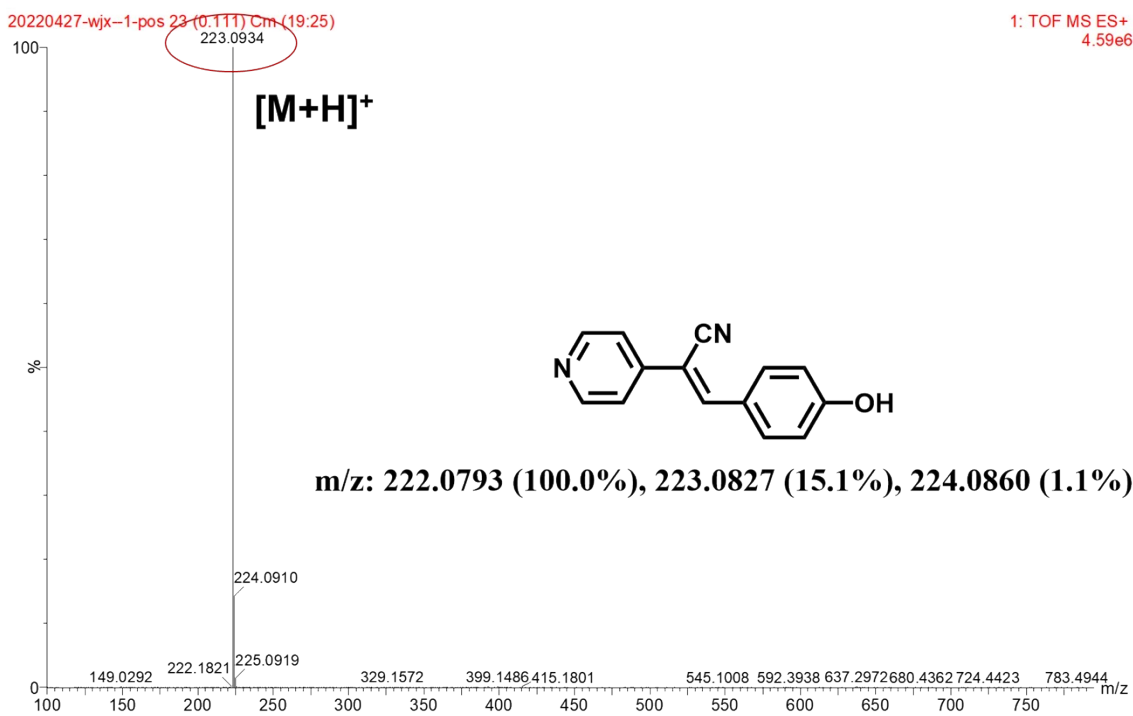
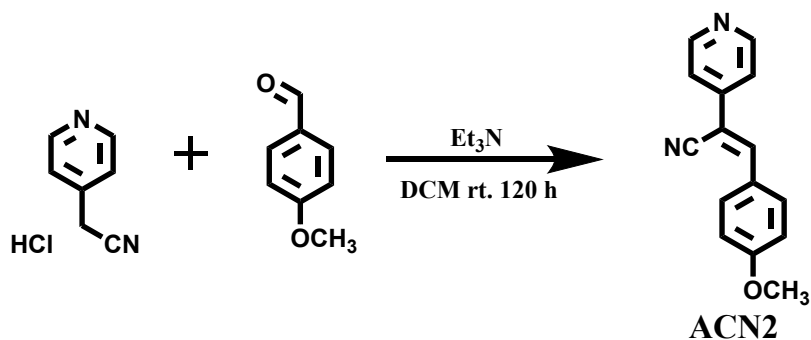
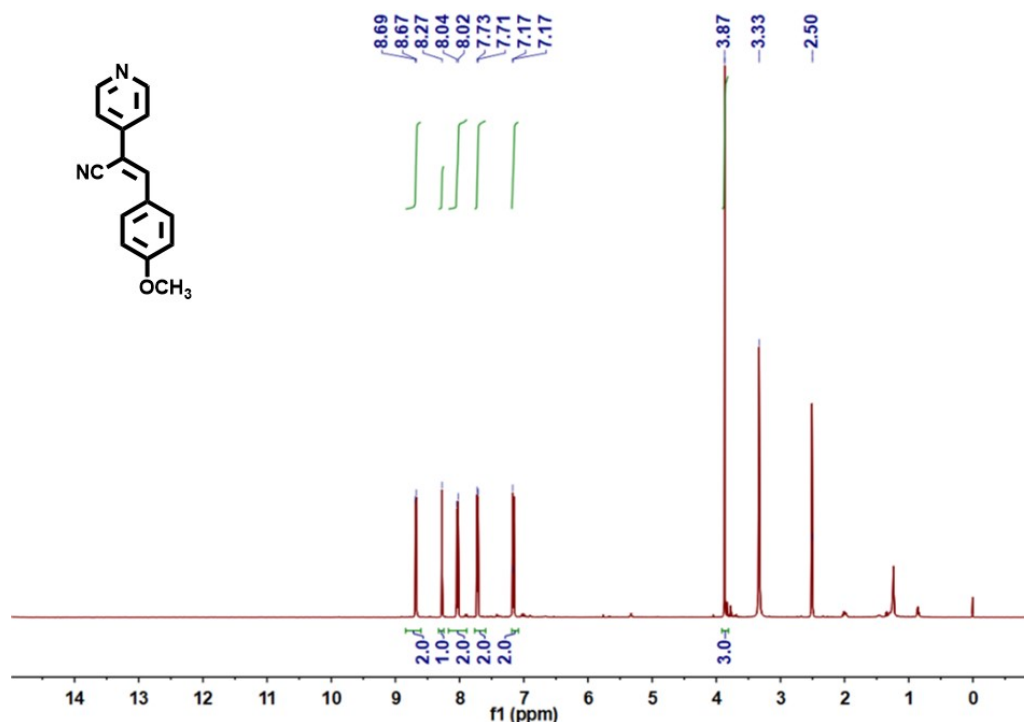


Figure S3. ESI-MS spectrum of ACN1.



**Scheme S2.** Structure and synthesis route to ACN2.

**Synthesis of (Z)-3-(4-methoxyphenyl)-2-(pyridin-4-yl)acrylonitrile (ACN2):** 4-Pyridylacetonitrile hydrochloride (0.3 g, 2 mmol), 4-Methoxybenzaldehyde (0.545 g, 4 mmol) and Et<sub>3</sub>N (1.5 mL, 10 mmol) were dissolved in 25 ml DCM under stirring at room temperature for 120 hours. After the stated time, the solvent was removed in vacuo and the residue was purified by flash chromatography on silica gel eluting with DCM/MeOH =100/3 mixtures. The yellow product is collected to give ACN2 (0.32 g, 1.5 mmol) in yield of 40%. <sup>1</sup>H NMR (400 MHz, DMSO-*d*<sub>6</sub>) δ 8.68 (d, J = 6.2 Hz, 2H), 8.27 (s, 1H), 8.03 (d, J = 8.9 Hz, 2H), 7.72 (d, J = 6.2 Hz, 2H), 7.17 (d, J = 1.8 Hz, 2H), 3.87 (s, 3H). <sup>13</sup>C NMR (101 MHz, DMSO) δ 162.42 (s), 150.89 (s), 146.11 (s), 141.97 (s), 132.36 (s), 126.10 (s), 120.01 (s), 118.02 (s), 115.16 (s), 114.26 (s), 104.95 (s), 56.03 (s). ESI-MS: Calculated mass: 236.0950; measured: 237.1141



**Figure S4.** <sup>1</sup>H NMR spectrum of ACN2 in DMSO-*d*<sub>6</sub>.

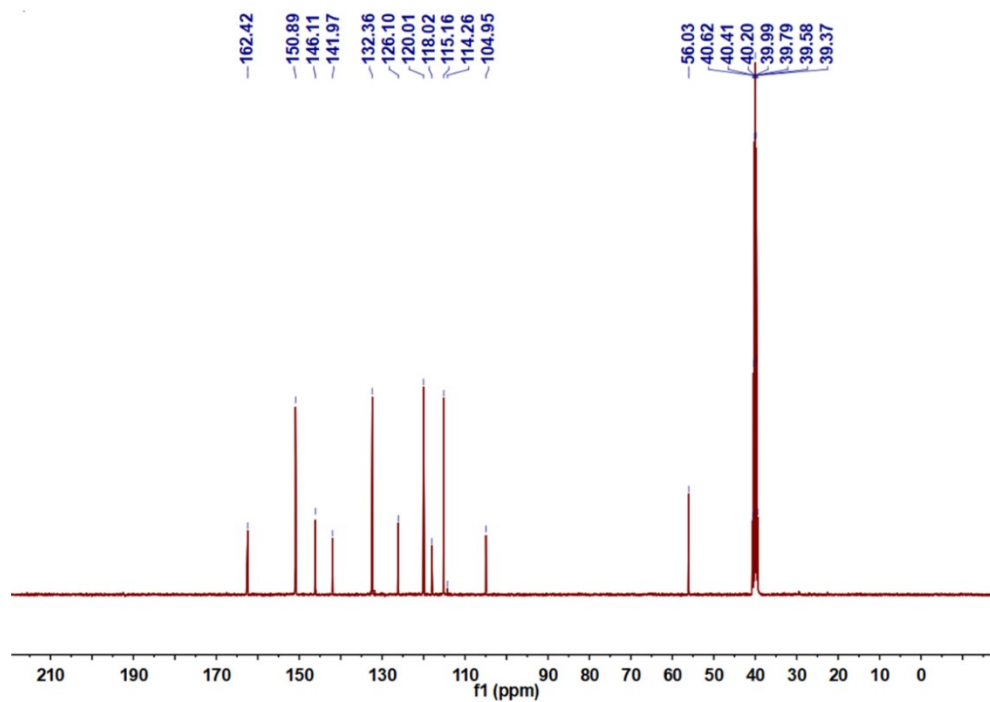


Figure S5.  $^{13}\text{C}$  NMR spectrum of ACN2 in  $\text{DMSO-d}_6$ .

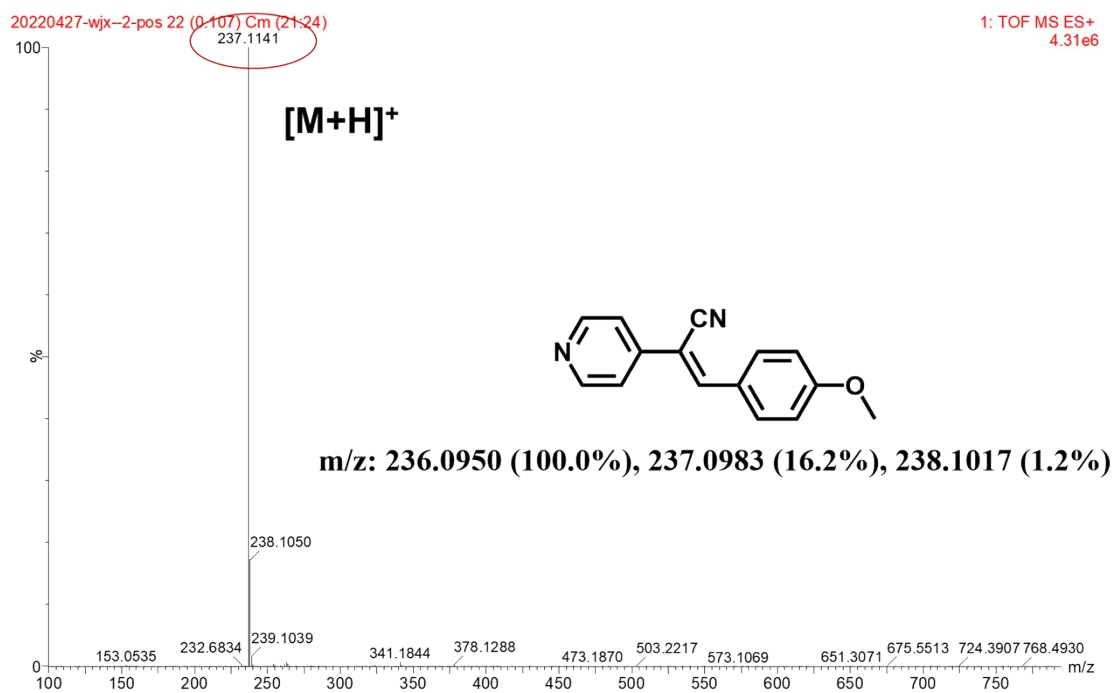
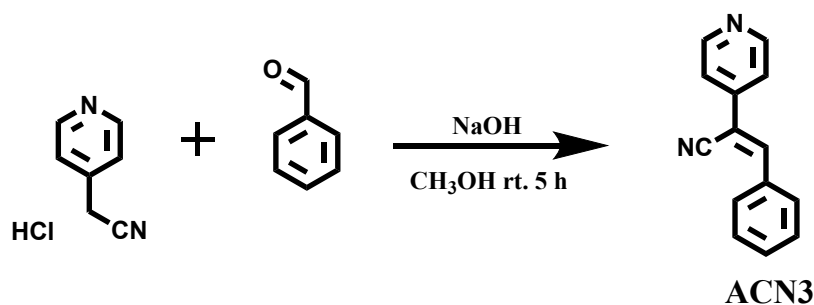
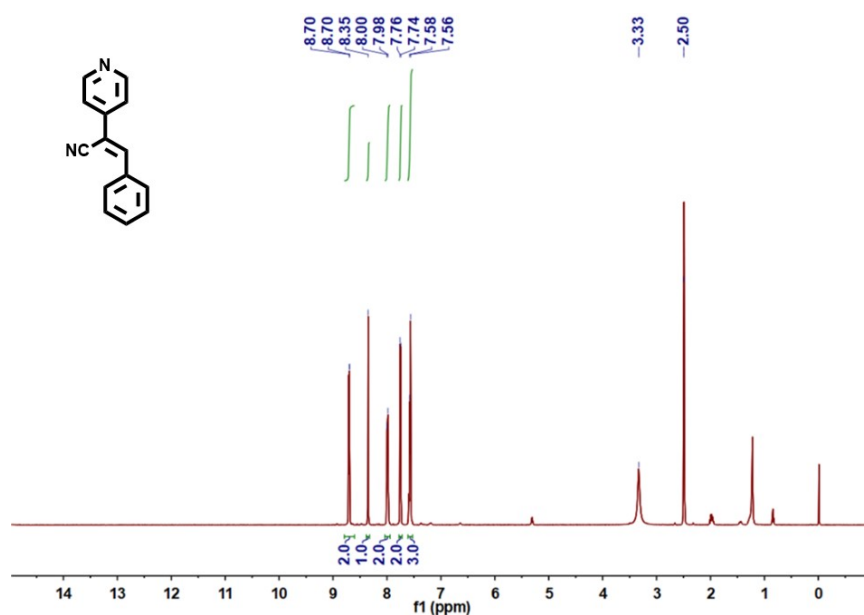


Figure S6. ESI-MS spectrum of ACN2.



**Scheme S3.** Structure and synthesis route to **ACN3**.

**Synthesis of (Z)-3-phenyl-2-(pyridin-4-yl)acrylonitrile (ACN3):** 4-Pyridylacetonitrile hydrochloride (0.2 g, 1.3 mmol), Benzaldehyde (0.18 g, 1.7 mmol) and NaOH (0.07 g, 2.0 mmol) in 40 ml of MeOH solution was stirred for 3 h at room temperature. After reaction, 100 ml of deionized water was poured into the reaction mixture. The precipitate was formed and filtered. After dryness, **ACN3** was collected as a red solid in yield of 60%.  $^1\text{H}$  NMR (400 MHz, DMSO- $d_6$ )  $\delta$  8.70 (dd,  $J = 4.7, 1.5$  Hz, 2H), 8.35 (s, 1H), 7.99 (dd,  $J = 7.4, 2.0$  Hz, 2H), 7.78-7.72 (m, 2H), 7.61-7.52 (m, 3H).  $^{13}\text{C}$  NMR (101 MHz, DMSO)  $\delta$  161.21 (s), 150.59 (s), 146.15 (s), 141.95 (s), 132.45 (s), 124.37 (s), 119.66 (s), 117.97 (s), 116.30 (s), 103.33 (s). ESI-MS: Calculated mass: 206.0844; measured: 206.1043



**Figure S7.**  $^1\text{H}$  NMR spectrum of **ACN3** in DMSO- $d_6$ .

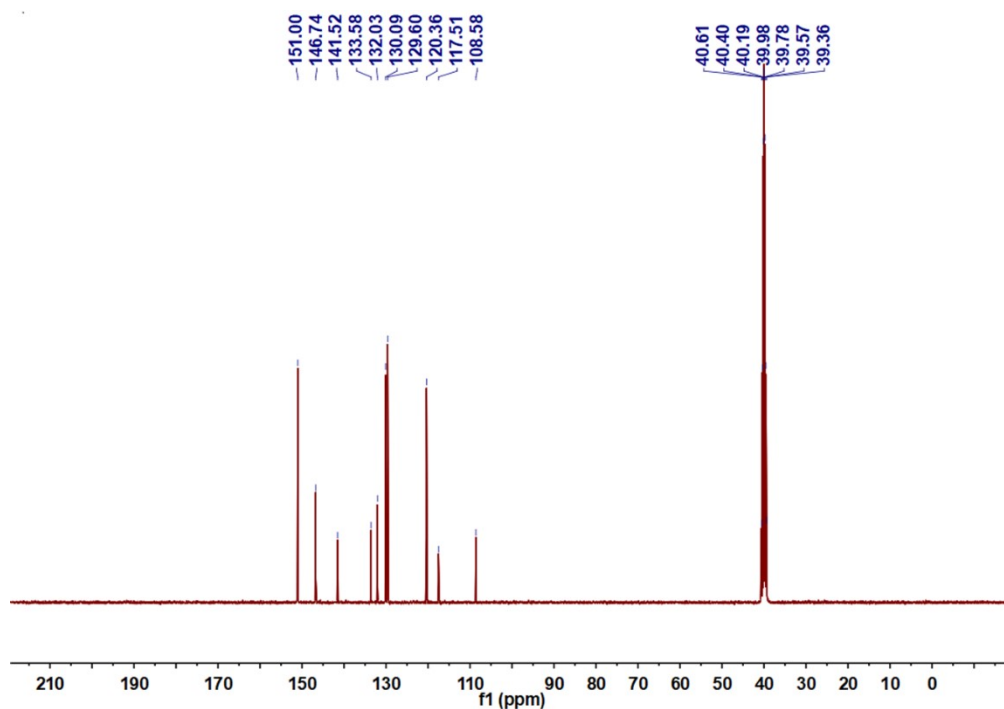


Figure S8.  $^{13}\text{C}$  NMR spectrum of ACN3 in  $\text{DMSO-d}_6$ .

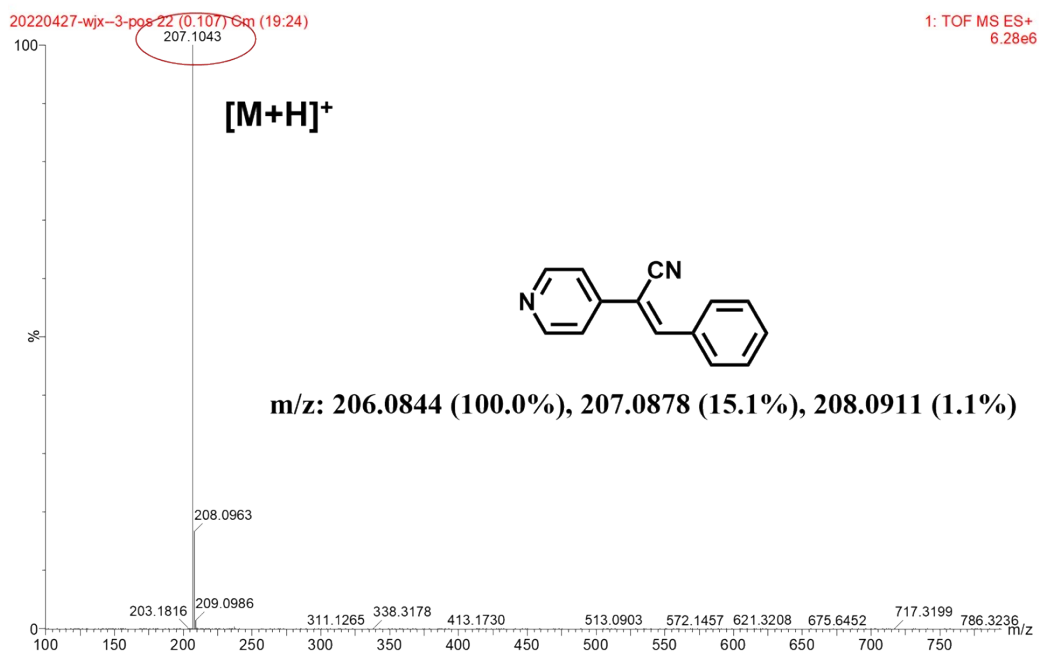
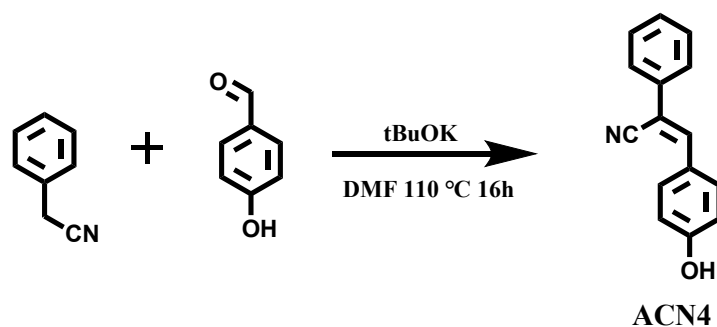


Figure S9. ESI-MS spectrum of ACN3.





**Scheme S4.** Structure and synthesis route to ACN4.

**Synthesis of (Z)-3-(4-hydroxyphenyl)-2-phenylacrylonitrile (ACN4):** Benzyl cyanide (0.12 g, 1 mmol), 4-Hydroxybenzaldehyde (0.18 mg, 1.5 mmol) DMF (1 ml) and 2 equivalents of tBuOK (0.225 g, 2 mmol) were added in a 10 mL tube equipped with a stirring bar under 110 °C for 16 h. When the reaction was completed, the reaction mixture was cooled to room temperature. The reaction was quenched with distilled water and the solution was extracted with ethyl acetate. The crude product was purified by column chromatography (DCM/ ethyl acetate = 50:1) and ACN4 in yield of 60%. <sup>1</sup>H NMR (400 MHz, DMSO-*d*<sub>6</sub>) δ 10.24 (s, 1H), 7.90 – 7.85 (m, 3H), 7.71 (d, *J* = 7.3 Hz, 2H), 7.49 (t, *J* = 7.6 Hz, 2H), 7.40 (t, *J* = 7.3 Hz, 1H), 6.91 (d, *J* = 8.7 Hz, 2H). <sup>13</sup>C NMR (101 MHz, DMSO-*d*<sub>6</sub>) δ 160.47 (s), 143.37 (s), 134.83 (s), 131.88 (s), 129.59 (s), 129.05 (s), 125.86 (s), 125.23 (s), 119.08 (s), 116.34 (s), 106.26 (s). ESI-MS: Calculated mass: 221.0841; measured: 222.0911.

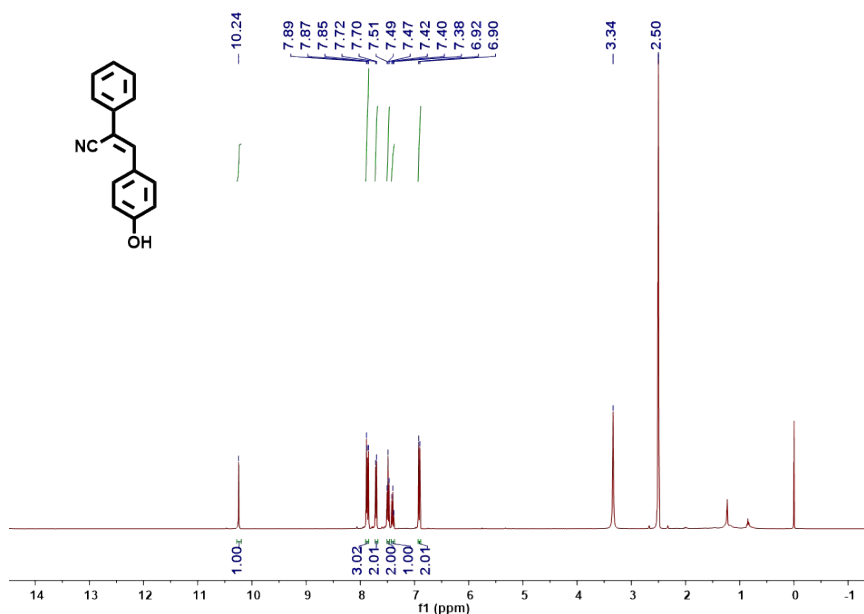


**Figure S10.** <sup>1</sup>H NMR spectrum of ACN4 in DMSO-*d*<sub>6</sub>.

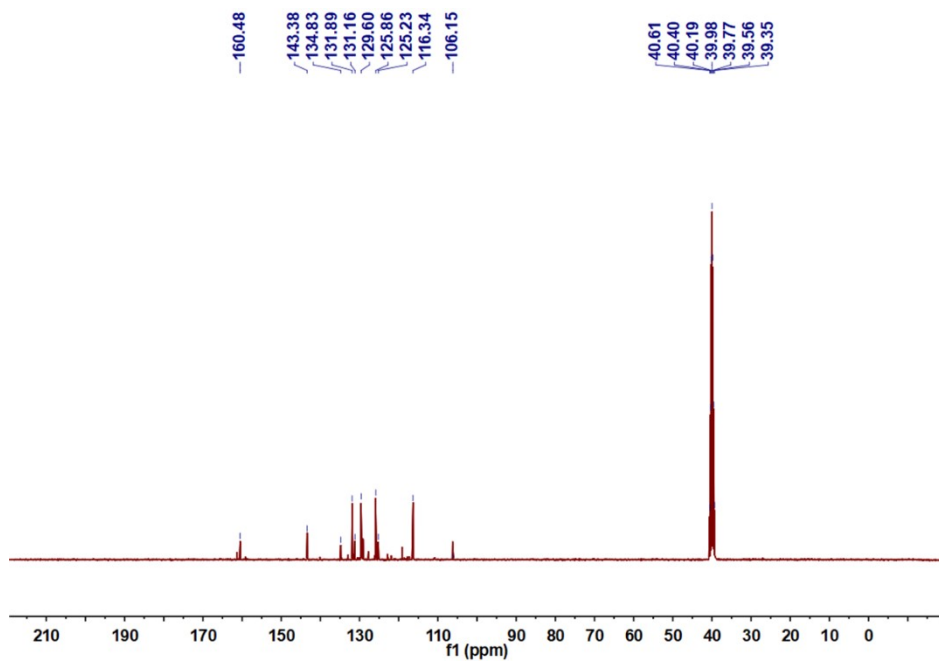


Figure S11.  $^{13}\text{C}$  NMR spectrum of ACN4 in  $\text{DMSO-d}_6$ .

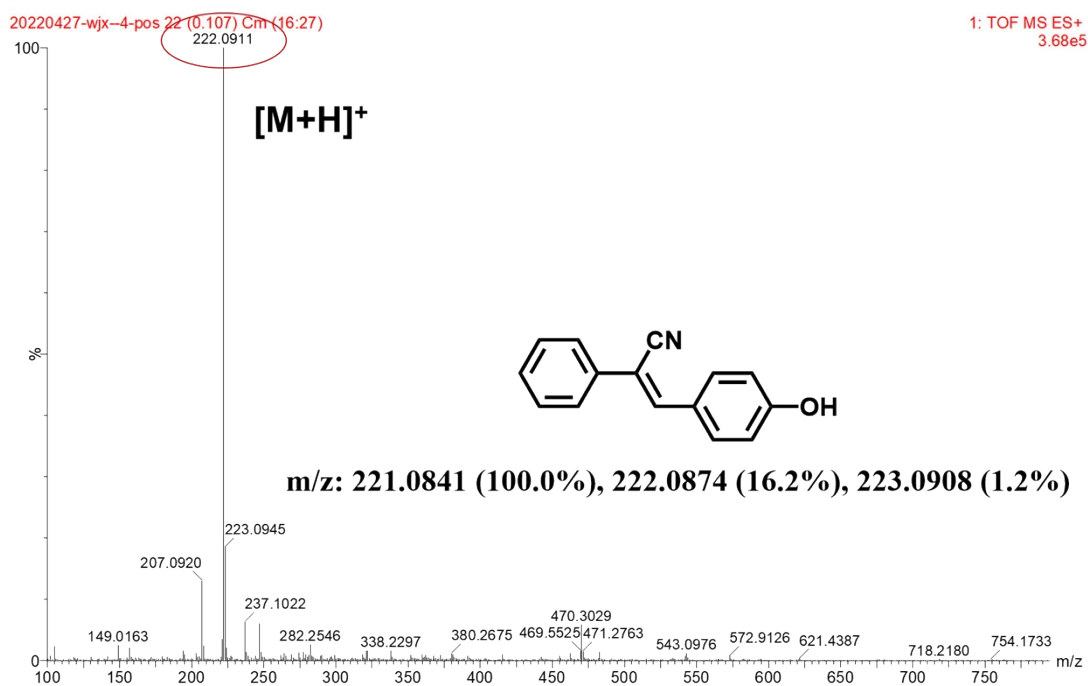
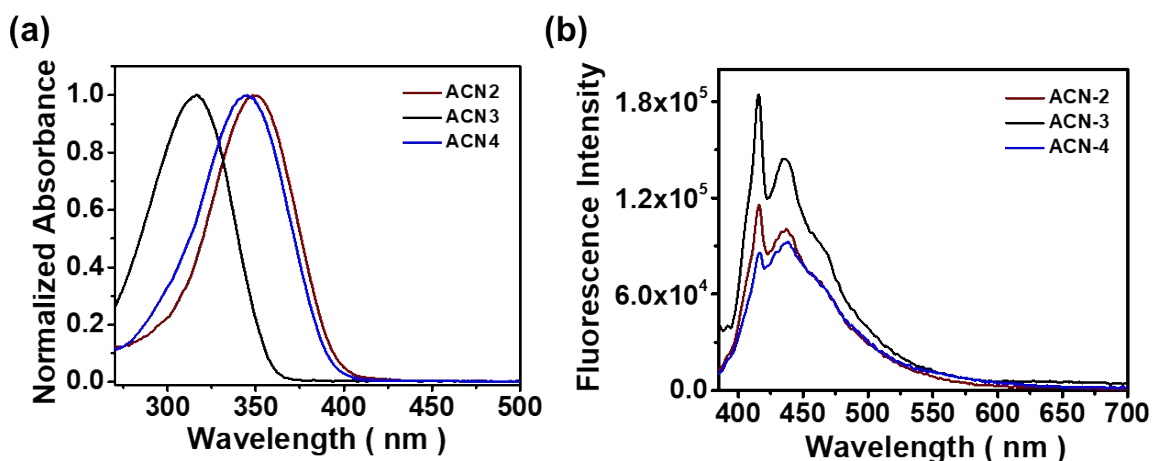


Figure S12. ESI-MS spectrum of ACN4.



**Figure S13.** (a) Normalized absorption spectra and (b) fluorescence spectra ( $\lambda_{\text{ex}} = 370$  nm) of ACN2,3,4,5 in DMSO solution ( $4 \times 10^{-5}$  M) at room temperature.

**Table S1.** Optical data of cyanostilbene derivatives ACN 1-5.

	Solution			Solid		
	$\lambda_a$ (nm)	$\lambda_f$ (nm)	$\Phi_f$	$\lambda_a$ (nm)	$\lambda_f$ (nm)	$\Phi_f$
ACN1	354	430	0.14	435/520	/	/
ACN2	350	436	0.23	400	505	1.52
ACN3	315	436	1.01	380/520	437/550	0.70
ACN4	345	445/560	0.09	420	480	0.85

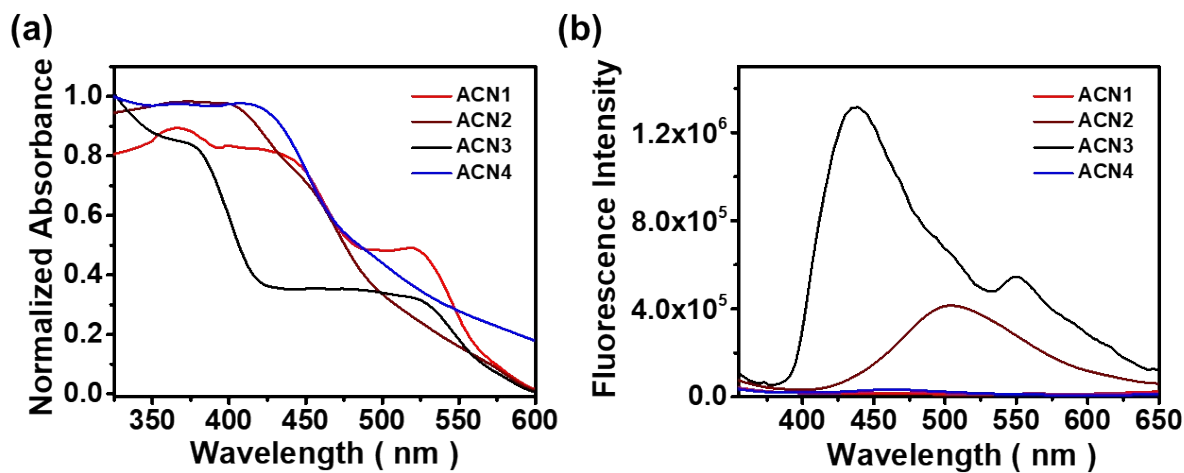


**Figure S14.** (a) UV-Vis absorption spectra and (b) fluorescence spectra ( $\lambda_{\text{ex}} = 340$  nm) of ACNs in the solid states.

**Table S2** Changes of the absorption peaks of ACN1-4.

compound	pH value of buffer solutions	Wavelength of the maximum absorption peaks (nm)
ACN1	2.0	385
	7.0	354
	13.0	415
ACN2	2.0	345
	7.0	380
ACN3	2.0	310
	7.0	340
ACN4	7.0	335
	13.0	385

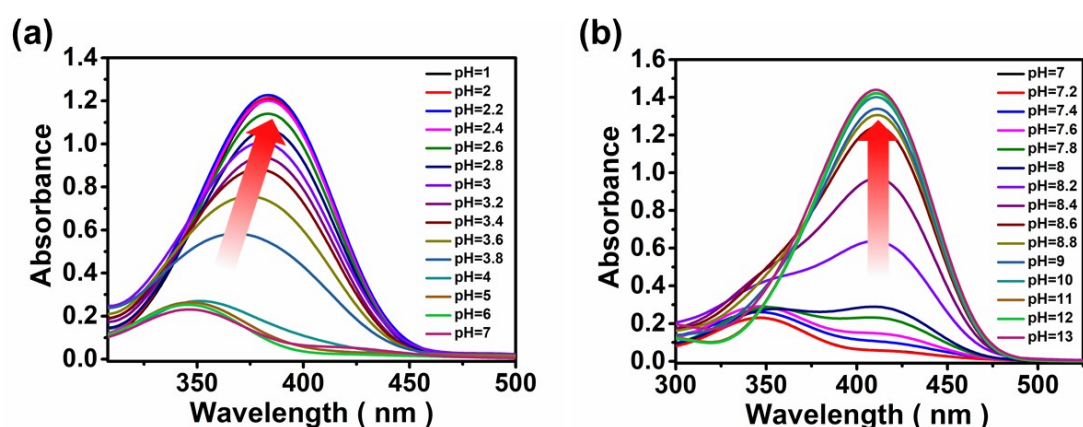


**Figure S15.** Absorption spectra of ACN1 ( $4 \times 10^{-5}$  M,  $V_{\text{DMSO}}: V_{\text{Buffer}} = 1:9$ ) in aqueous solutions with different pH values.: (a) pH 1.0-7.0, (b) pH 7.0-13.0.

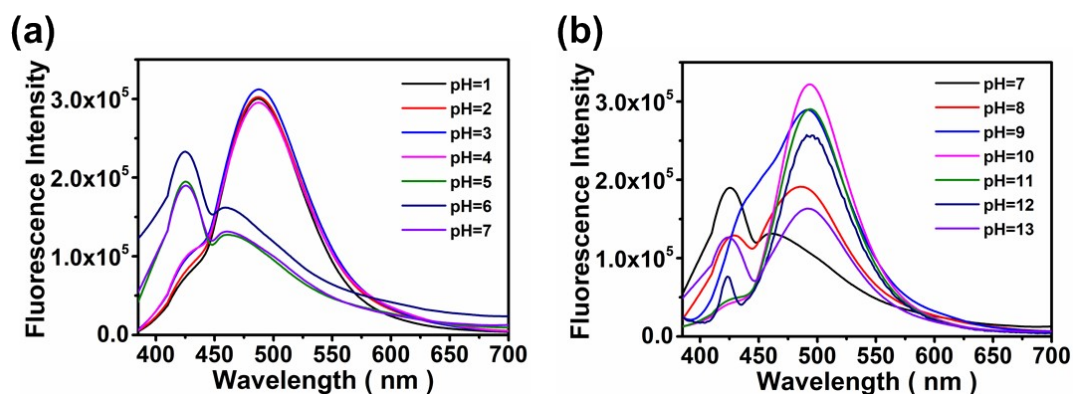


**Figure S16.** Fluorescence spectra ( $\lambda_{\text{ex}} = 370$  nm) of ACN1 ( $4 \times 10^{-5}$  M,  $V_{\text{DMSO}}: V_{\text{Buffer}} = 1:9$ ) in buffer aqueous solutions: (a) pH = 1.0-7.0, (b) pH = 7.0-13.0.

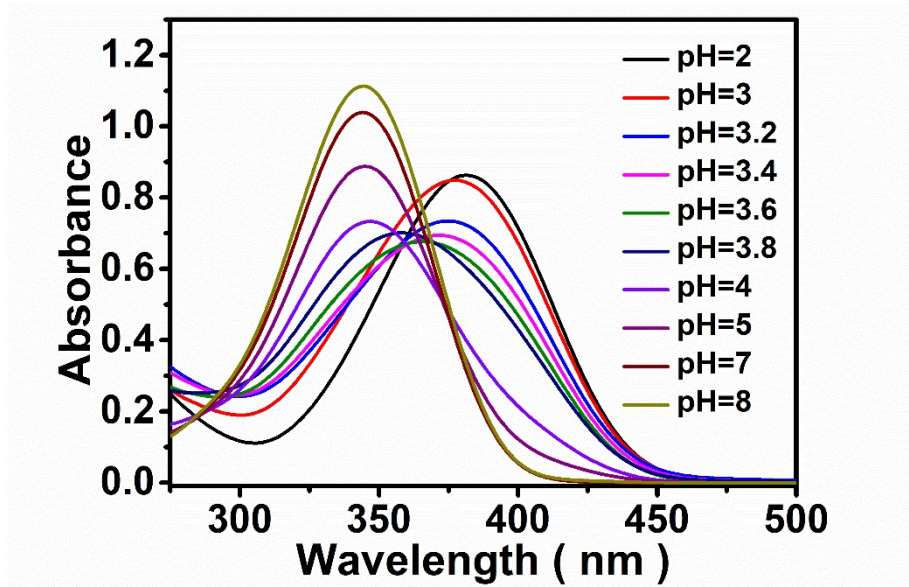


**Figure S17.** Absorption spectra of ACN2 ( $4 \times 10^{-5}$  M,  $V_{\text{DMSO}} : V_{\text{Buffer}} = 1:9$ ) in aqueous solutions with different pH values.

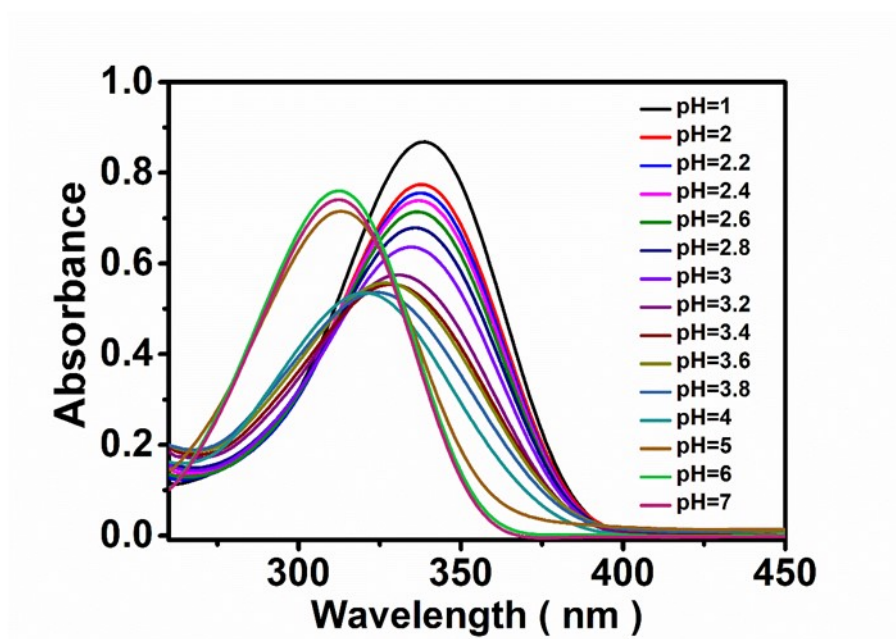


**Figure S18.** Absorption spectra of ACN3 ( $4 \times 10^{-5}$  M,  $V_{\text{DMSO}} : V_{\text{Buffer}} = 1:9$ ) in aqueous solutions with different pH values.

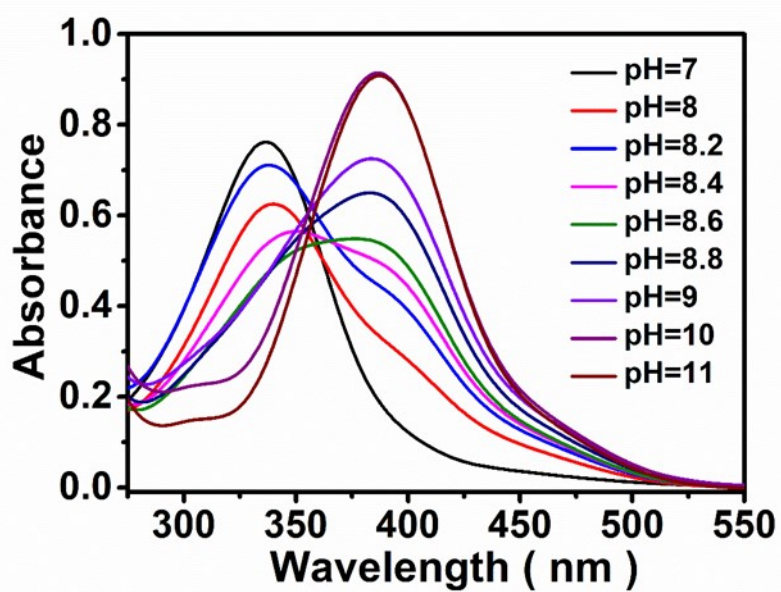


**Figure S19.** Absorption spectra of ACN4 ( $4 \times 10^{-5}$  M,  $V_{\text{DMSO}}:V_{\text{Buffer}}=1:9$ ) in aqueous solutions with different pH values.

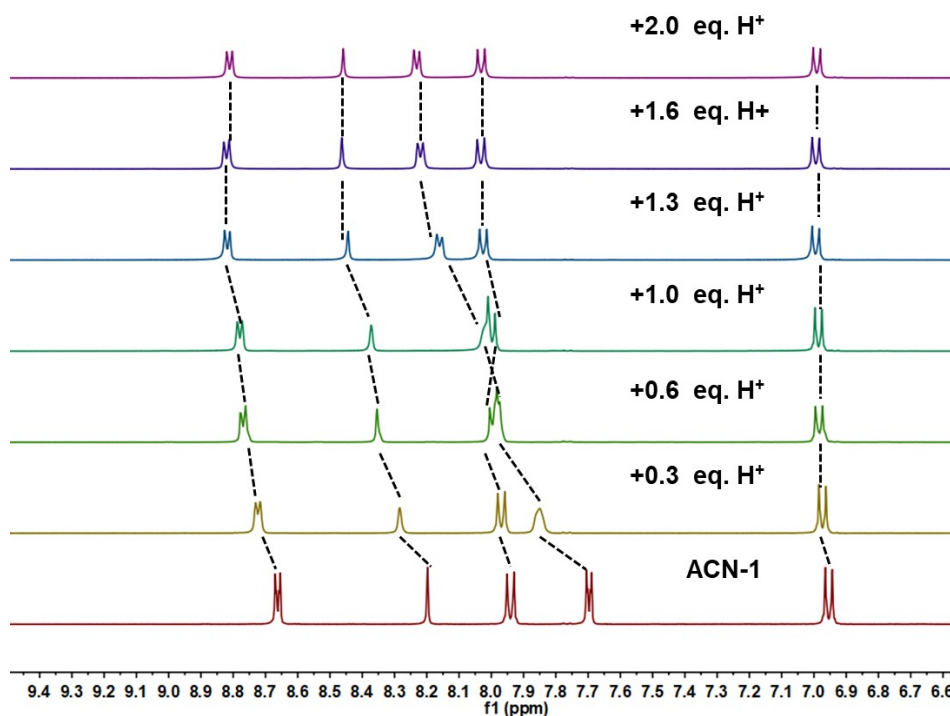


**Figure S20.**  $^1\text{H}$  NMR spectra of the titration experiment of ACN1 response to different amounts of DCl (DMSO- $d_6$ , from up to down: 0, 0.3, 0.6, 1.0, 1.3, 1.6 and 2.0 equiv. of DCl).

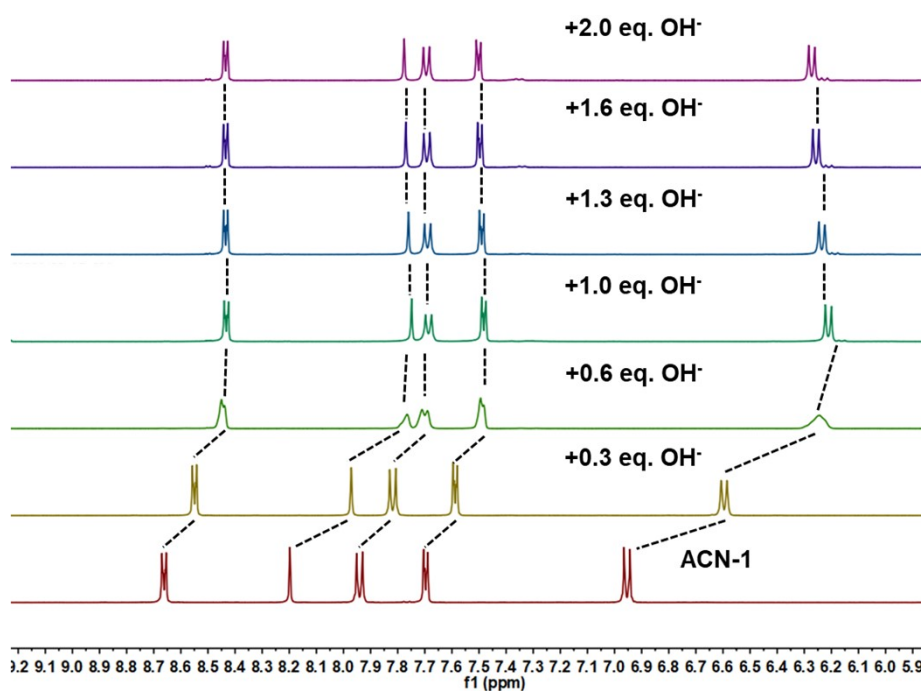


**Figure S21.**  $^1\text{H}$  NMR spectra of the titration experiment of ACN1 response to different amounts of NaOD (DMSO- $\text{d}_6$ , from up to down: 0, 0.3, 0.6, 1.0, 1.3, 1.6 and 2.0 equiv. of NaOD).

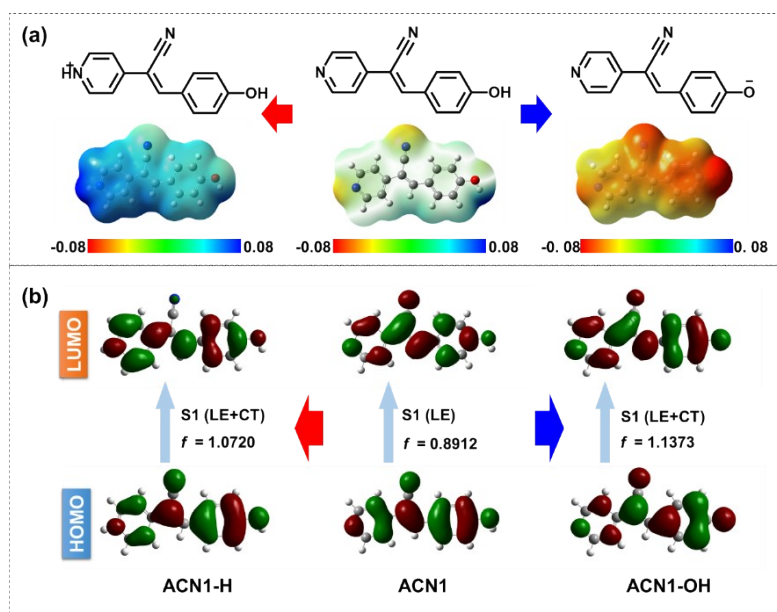


**Figure S22.** (a) Electrostatic potential surfaces of ACN1, ACN1-H and ACN1-OH. (b) HOMOs and LUMOs of the  $S_0$ - $S_1$  transitions of ACN1, ACN1-H and ACN1-OH.

**Table S3.** Calculated energy levels and electronic transition characters of the singlet states of ACN1, ACN1-H and ACN1-OH.

	Excite State	Energy	Wavelength	Oscillator Strengths	Transitions	Excitation Type	Ratio
ACN1	S1	3.85 eV	382 nm	$f=0.8912$	H→L	LE	97.2%
	S4	4.89 eV	253 nm	$f=0.0251$	H-1→L	LE+CT	74.7%
ACN1-H	S1	3.12 eV	397 nm	$f=1.0720$	H→L	LE+CT	96.0%
	S3	4.49 eV	276 nm	$f=0.0141$	H-3→L	CT	2.5%
					H-2→L+1		6.5%
S4	4.88 eV	254 nm	$f=0.0426$	H-2→L H→L+1	LE+CT	82.2% 8.6%	
ACN1-OH	S1	3.09 eV	400 nm	$f=1.1373$	H→L	LE+CT	96.0%
	S4	4.18 eV	297 nm	$f=0.0740$	H-2→L+2 H→L+2	CT	5.5% 88.5%

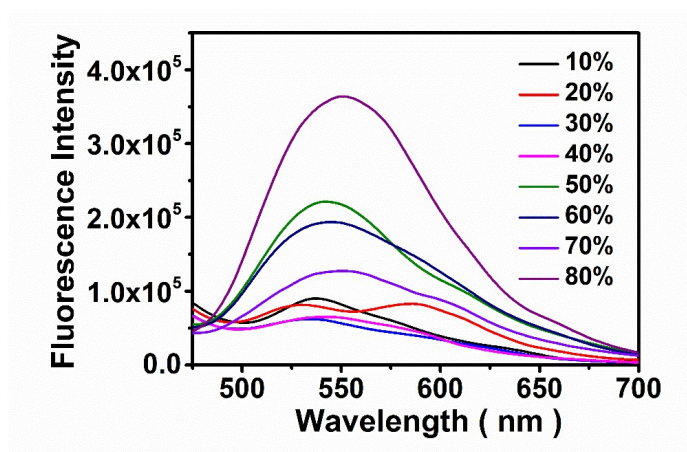


**Figure S23.** Fluorescence spectra ( $\lambda_{\text{ex}} = 370$  nm) of ACN1 treated with acid solution in THF/Hexane mixtures with different Hexane fraction ( $f_{\text{Hex}}$ ), concentration:  $4 \times 10^{-5}$  M.

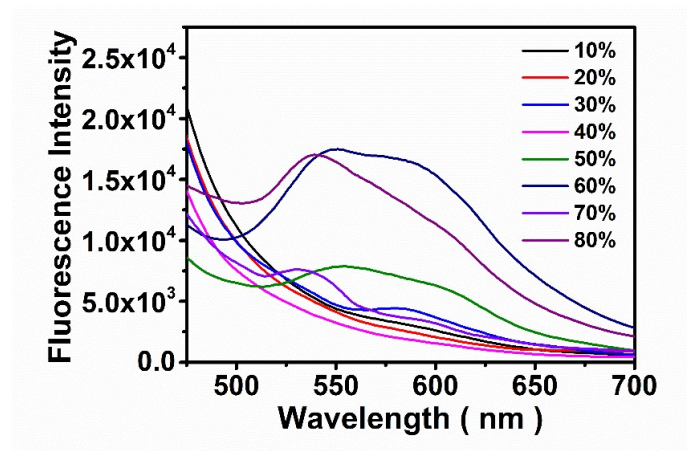


**Figure S24.** Fluorescence spectra ( $\lambda_{\text{ex}} = 370$  nm) of ACN1 treated with base solution in THF/Hexane mixtures with different Hexane fraction ( $f_{\text{Hex}}$ ), concentration:  $4 \times 10^{-5}$  M.



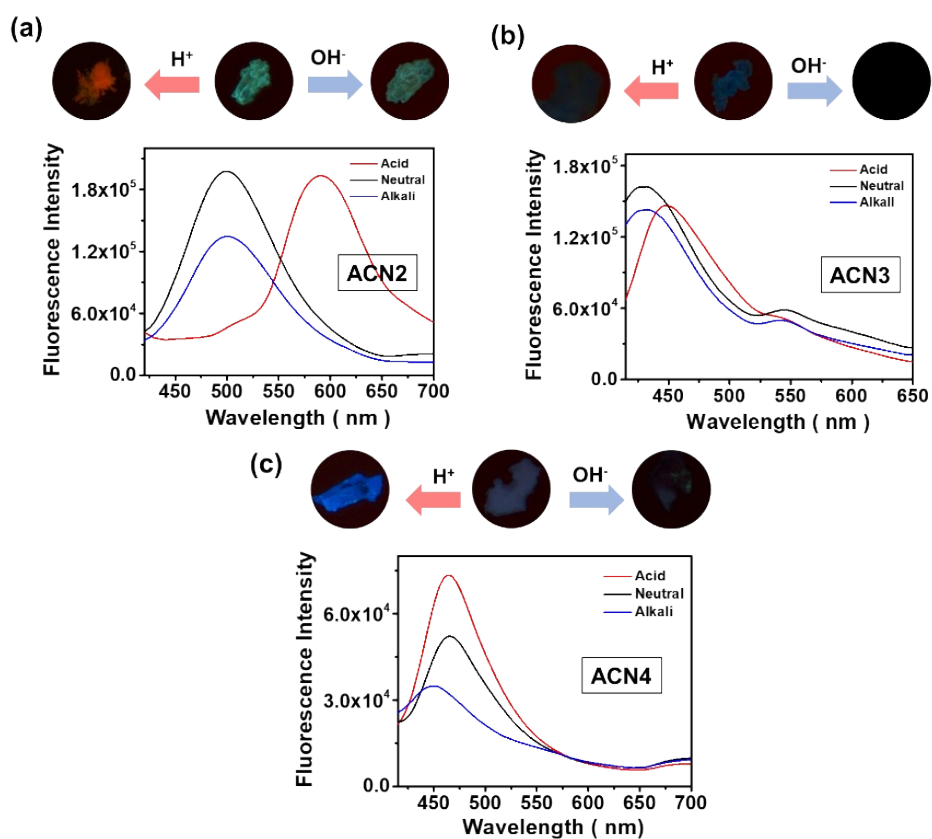


**Figure S25.** Fluorescence photographs and spectra ( $\lambda_{\text{ex}} = 370 \text{ nm}$ ) (a) ACN2 (b) ACN3 (c) ACN4 solid powder after acid/base treatment.

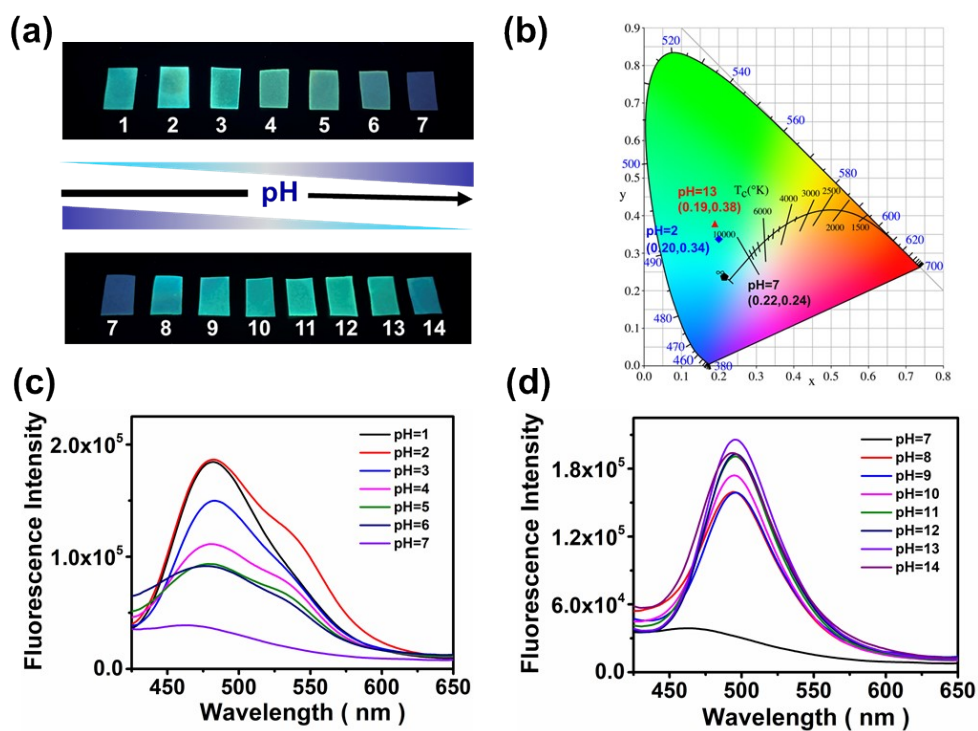


**Figure S26.** (a) Fluorescence photographs of FP1 after detecting different pH solutions. (b) CIE coordinate diagram for FP1 under pH=2.0 and pH=13.0. FL spectra ( $\lambda_{\text{ex}} = 370 \text{ nm}$ ) of test paper in (c) acid and (d) base pH conditions.

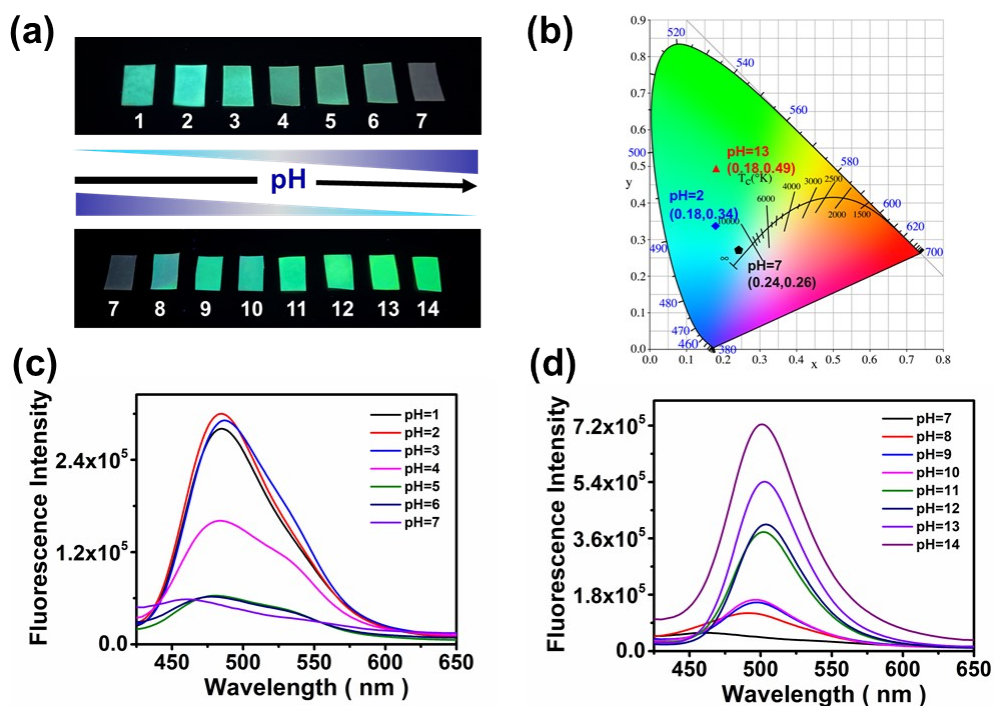


**Figure S27.** (a) Fluorescence (FL) photos of FP1H after detecting different pH solutions. (b) CIE coordinate diagram for FP1H under pH=2.0 and pH=13.0. Fluorescence spectra ( $\lambda_{\text{ex}} = 370 \text{ nm}$ ) of test paper in (c) acid and (d) base conditions.

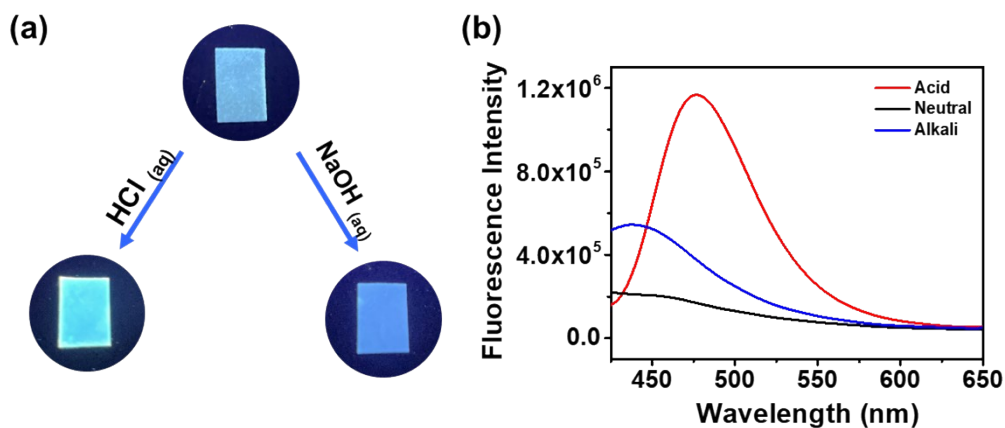


**Figure S28.** (a) Fluorescence photos and (b) spectra ( $\lambda_{\text{ex}} = 370 \text{ nm}$ ) of FP2 after treated by acid and base solutions.

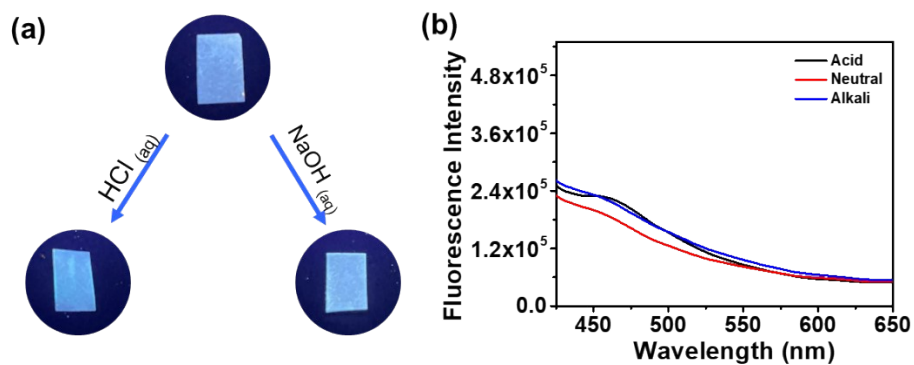


**Figure S29.** (a) Fluorescence photos and (b) spectra ( $\lambda_{\text{ex}} = 370$  nm) of **FP3** after treated by acid or base solution.

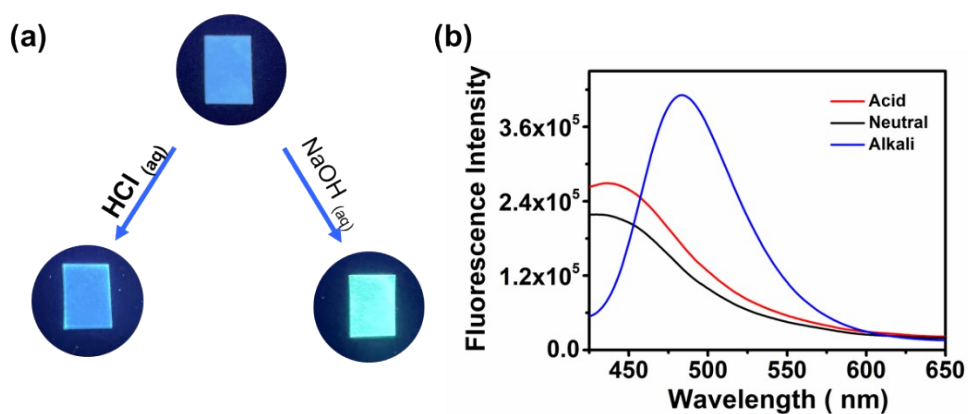


**Figure S30.** (a) Fluorescence photos and (b) spectra ( $\lambda_{\text{ex}} = 370$  nm) of **FP4** after treated by acid or base solution.

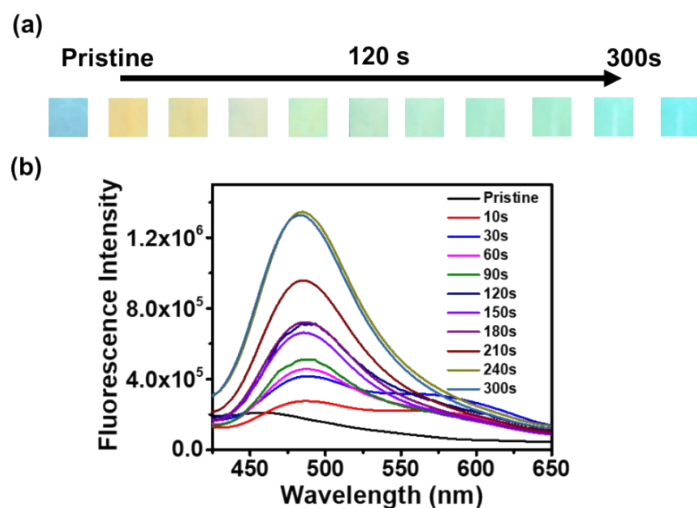


**Figure S31.** Time-dependent fluorescence photos and fluorescence spectra ( $\lambda_{\text{ex}} = 370$  nm) of **FP1H** under fuming with HCl vapors.

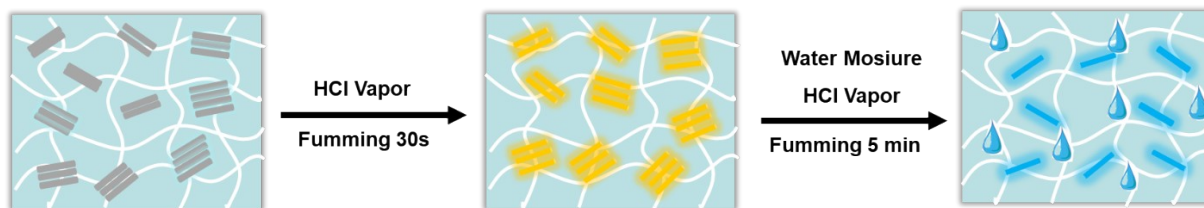


**Figure S32.** Schematic diagram of fluorescence changes under HCl fuming for different times.

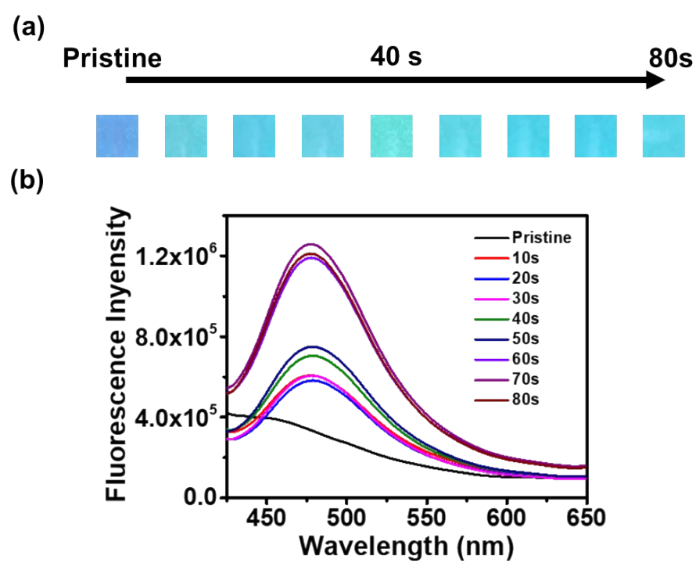


**Figure S33.** Time-dependent fluorescence photos and fluorescence spectra ( $\lambda_{\text{ex}} = 370 \text{ nm}$ ) of **FP1** under fuming with HCl vapors.

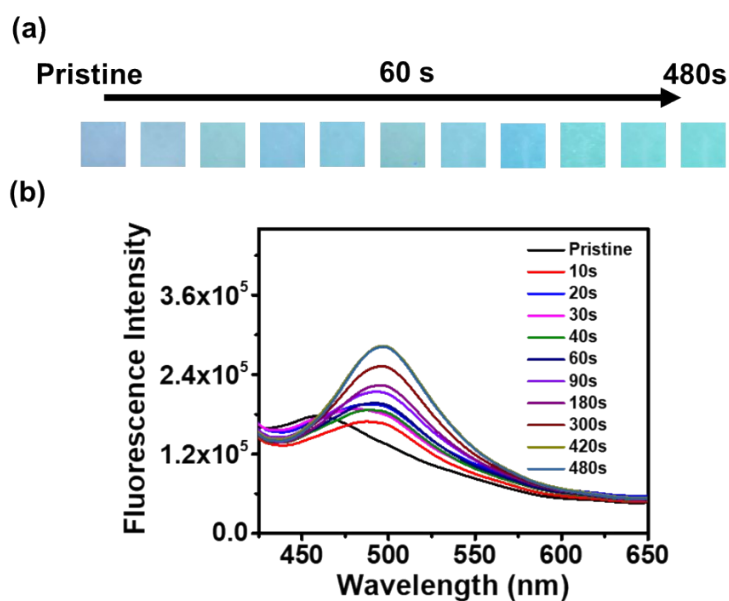


**Figure S34.** Time-dependent fluorescence photos and fluorescence spectra ( $\lambda_{\text{ex}} = 370 \text{ nm}$ ) of **FP1H** under fuming with  $\text{NH}_3$  vapors.

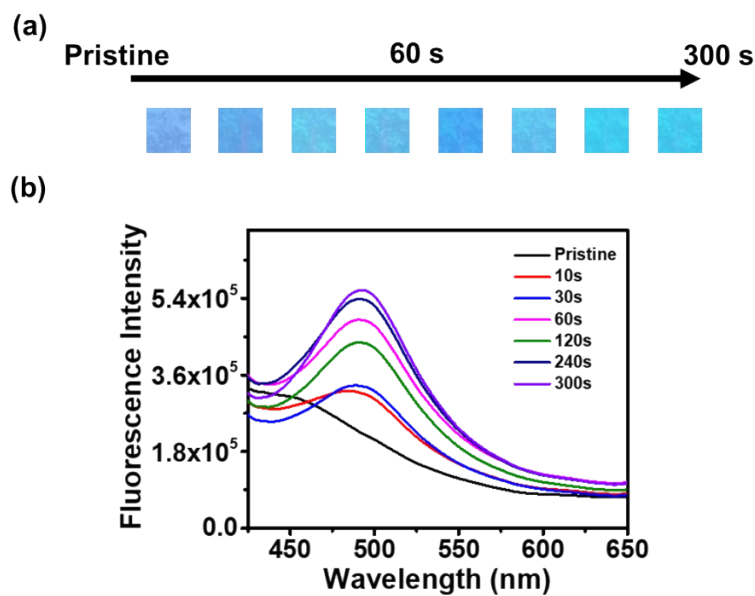


**Figure S35.** Time-dependent fluorescence photos and fluorescence spectra ( $\lambda_{\text{ex}} = 370 \text{ nm}$ ) of **FP1** under fuming with  $\text{NH}_3$  vapors.



**Figure S36.** Paper anti-counterfeiting using (a) acid or (b) base solution as security inks. Fluorescent patterns of “BUCT” are observed on FP1H under UV light and after placing for 15 days.

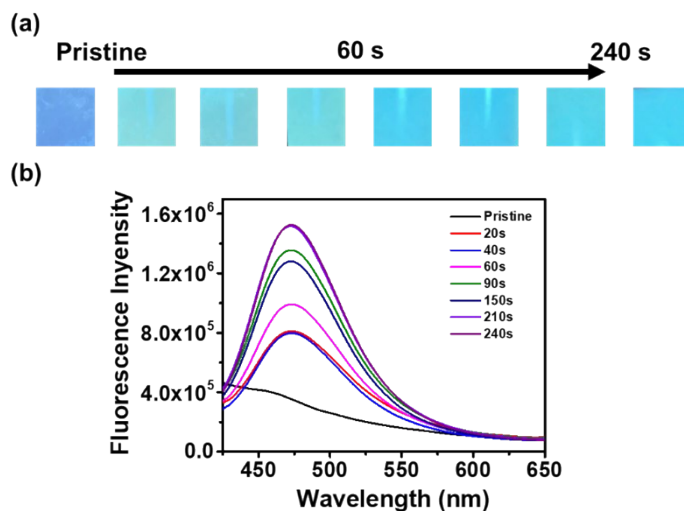


**Figure S37.** Time-dependent fluorescence photos and fluorescence spectra ( $\lambda_{\text{ex}} = 370 \text{ nm}$ ) of **FP2** fuming with  $\text{HCl}$  vapors.

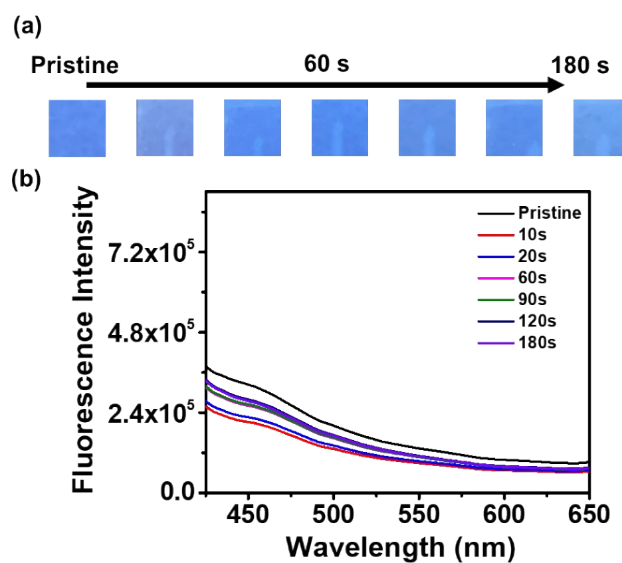


**Figure S38.** Time-dependent fluorescence photos and fluorescence spectra ( $\lambda_{\text{ex}} = 370 \text{ nm}$ ) of **FP3** fuming with HCl vapors.

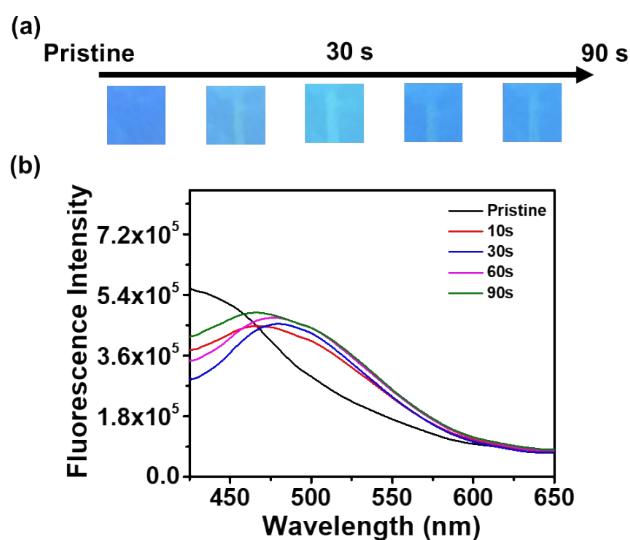


**Figure S39.** Time-dependent fluorescence photos and fluorescence spectra ( $\lambda_{\text{ex}} = 370 \text{ nm}$ ) of **FP4** fuming with  $\text{NH}_3$  vapors.

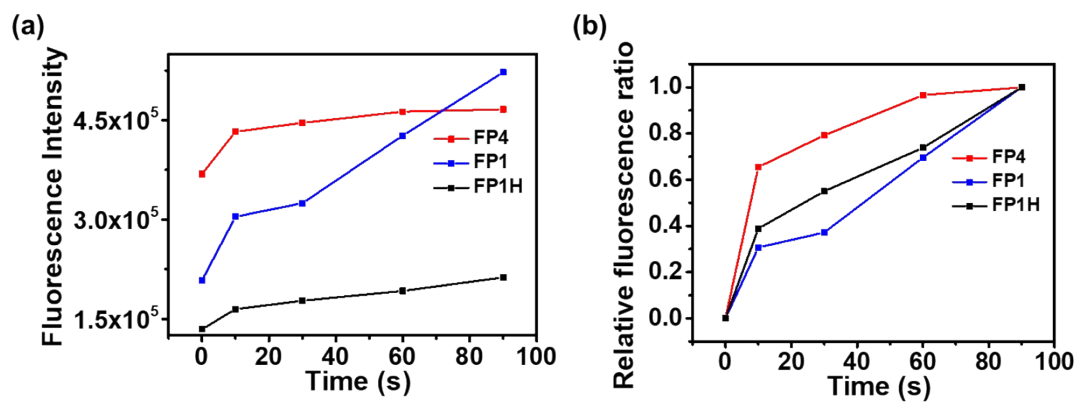


**Figure S40.** (a) Fluorescence changes and (b) changes in fluorescence ratio of FP4 (red line), FP1 (blue line) and FP1H (black line) under the fumigation of  $\text{NH}_3$  vapor.